

CD151 Gene Delivery after Myocardial Infarction Promotes Functional Neovascularization and Activates FAK Signaling

Houjuan Zuo,¹ Zhengxiang Liu,¹ Xiaochun Liu,² Jun Yang,³ Tao Liu,¹ Sha Wen,¹ Xin A Zhang,⁴ Katherine Cianflone,⁵ and Daowen Wang¹

¹Department of Cardiology of Tongji Hospital, Tongji Medical College, Huazhong University of Science and Technology, Wuhan, China; ²Department of Neurobiology, Tongji Medical College, Huazhong University of Science and Technology, Wuhan, China; ³Department of Cardiology of Yuhuangding Hospital, Qingdao Medical College, Qingdao University, Yantai, China; ⁴Vascular Biology Center, Cancer Institute, and Departments of Medicine and Molecular Science, University of Tennessee Health Science Center, Tennessee, United States of America; ⁵Centre de Recherche Laval Hospital, Laval University, Quebec, Canada

Our previous studies showed that tetraspanin CD151 promotes neovascularization in rat hindlimb and myocardial ischemia models. This study is to assess whether *CD151* induces arteriogenesis and promotes functional neovascularization in a pig myocardial infarction model, and to determine the signaling pathways involved. *CD151* cDNA and *antiCD151* sequence were constructed into a recombinant adeno-associated virus (rAAV) vector. All 26 pigs used either were subjected to coronary artery ligation or did not undergo surgery. Eight wks after viral administration, the expression of CD151 protein was measured by Western blot. The densities of capillaries and arterioles were determined using immunohistochemistry. Regional myocardial perfusion and other myocardial functions were evaluated by ¹³N-labeled NH₃ positron emission computed tomography (¹³N-NH₃ PET) and echocardiography. Western blot was performed for assessing the signaling mechanisms. Overexpression of CD151 markedly increased the densities of capillaries and arterioles, significantly enhanced the regional myocardial perfusion, reduced myocardial ischemia, and improved the myocardial contraction, wall motion, and wall thickness. Conversely, *antiCD151* gene delivery reversed the above changes. In addition, CD151 activated focal adhesion kinase (FAK), extracellular signal-regulated kinase (ERK), c-Jun N-terminal kinase (JNK), phosphatidylinositol-3 kinase (PI3K), protein kinase B (Akt), and endothelial nitric-oxide synthase (eNOS), and increased nitric oxide (NO) level. These findings demonstrate a robust role of CD151 in inducing and/or upregulating neovascularization. CD151-dependent neovascularization correlates with the activations of FAK, mitogen activated protein kinases (MAPKs), and PI3K signaling, suggesting that CD151 may promote neovascularization via MAPKs and PI3K pathways.

© 2009 The Feinstein Institute for Medical Research, www.feinsteininstitute.org

Online address: <http://www.molmed.org>

doi: 10.2119/molmed.2009.00025

INTRODUCTION

Myocardial ischemia is one of the most promising targets of gene therapy (1). Therapeutic angiogenesis aims to induce the formation of new blood vessels by delivering growth factors. Angiogenesis is the growth or sprouting of new capillaries from preexisting blood vessels which lack vascular smooth muscle cells (2,3). However, increasing evidence indicates that an-

giogenesis response is unlikely to contribute to the improvement the regional blood flow, as angiogenesis includes mainly new capillary blood vessels which are fragile and prone to rupture, and are unable to sustain proper circulation (2,4). In the case of occlusion of a major artery (coronary artery, and so on), preexisting arteriolar connections can be recruited to bypass the site of occlusion and arterio-

genesis would occur. Arteriogenesis is the formation of arterioles, the remodeling of preexisting vessels into larger collateral arteries (1,2). Arteriogenesis is reported to be the mature form of new vessels and is able to provide enhanced perfusion. So, one major challenge of gene therapy is to induce an arteriogenesis response, leading to an efficient restoration of blood flow (1,2,5).

CD151, a tetraspanin superfamily protein, contains two extracellular loops, four hydrophobic transmembrane domains, and two short cytoplasmic tails (6,7). This tetraspanin is expressed broadly in various cell types and, characteristically, localized at perinuclear vesicles and cell-cell junctions in endothelial cells (ECs) (8,9). Functional studies have revealed a role for CD151 in regulating EC motility and

Address correspondence and reprint requests to Zhengxiang Liu, Department of Cardiology of Tongji Hospital, Tongji Medical College, Huazhong University of Science and Technology, Wuhan 430030, China. Phone: 86-027-8366-2601; Fax: 86-027-8366-2622; E-mail: liuzhengxiang@hotmail.com.

Submitted May 30, 2009; Accepted for publication June 4, 2009; Epub (www.molmed.org) ahead of print June 18, 2009.

in vitro angiogenesis (9–11). A recent study demonstrates that the mouse lung endothelial cells (MLECs) from CD151 null mice display marked reduction in the angiogenesis-related endothelial events including migration, spreading, invasion, Matrigel contraction, tube and cable formation, and spheroid sprouting (12). In parallel, transfection of *CD151* cDNA into human umbilical vein ECs enhances cell proliferation, migration, and capillary tube formation on Matrigel (13). All these characteristics of CD151 strongly suggest that it can be useful for gene therapy to target myocardial ischemia by promoting angiogenesis. We have reported that *CD151* gene delivery increases the number of microvessels in a rat myocardial ischemia model and a rat ischemic hindlimb model (14–15). Although CD151 is an important promoter for angiogenesis both *in vitro* and *in vivo*, it remains to be determined whether CD151 also induces the arteriogenesis response.

Previous studies have established that CD151 specifically binds to integrins such as $\alpha 3\beta 1$, $\alpha 6\beta 1$, and $\alpha 6\beta 4$ (9,16–17). A primary role of CD151 is regulating integrin activity and function. For example: CD151 increases the activity of $\alpha 3\beta 1$ -integrin binding to laminin through stabilization of its activated conformation (18); CD151 strengthens $\alpha 6\beta 1$ integrin-mediated adhesion to laminin-1 (16). In addition to the integrin association, CD151 links to signaling enzymes such as phosphatidylinositol-4 kinase and protein kinase C (17,19). Moreover, CD151 also is reported to form a structural and functional complex with hepatocyte growth factor (HGF) receptor c-Met, acting as a molecular controller for the HGF/c-Met signaling pathway (20). Therefore, CD151 modifies integrin-mediated outside-in signaling and may transduce its own signals through formation of multimolecular complexes with other membrane proteins (19–21). Few studies have explored the molecular mechanisms of CD151 in angiogenesis (13,15,22). Further, the explicit signaling mechanism by which CD151 regulates blood vessel formation and maintenance has not been well elucidated.

Large animal models are necessary for research on gene therapy approaches (1). In the present study, we chose a porcine model for gene transduction. We used a strategy of direct intramyocardial administration of a recombinant adeno-associated virus (rAAV) construct coding CD151 in pigs with coronary ligation. An antiCD151 was constructed using antisense nucleic acid technique to downregulate the expression of CD151. The purpose of this study was to evaluate whether CD151 induces angiogenesis and arteriogenesis, and to determine the signaling pathways involved. We showed that focal adhesion kinase (FAK), mitogen-activated protein kinases (MAPKs), and phosphatidylinositol-3-kinase (PI3K) signaling pathways played differential roles in CD151 signal transduction.

MATERIALS AND METHODS

Plasmids and Antibodies

The pZeoSV-CD151 plasmid was described in an earlier study (13,14). Anti-CD151(sc-18753), anti-von Willebrand factor (vWF), (sc-73268) anti-FAK (sc-558), anti-phospho-FAK925 (sc-101680), anti-PI3K (sc-1404), anti-Akt (sc-5298), anti-phospho-Akt (sc-101629), anti-p38MAPK (sc-535), anti-phospho-p38MAPK (sc-7973), anti-c-Jun N-terminal kinase (JNK) (sc-571), anti-phospho-JNK (sc-6254), anti-c-Jun (sc-1694), anti-phospho-c-Jun (sc-7981), anti- β -actin (sc-47778), and anti-smooth muscle (SM) α -actin (sc-130616), anti-extracellular signal-regulated kinase (ERK) (sc-94), and anti-phospho-ERK (sc-16982) antibodies were purchased from Santa Cruz Biotechnology (Santa Cruz, CA, USA). Anti-phospho-FAK397 (44624G), anti-phospho-endothelial nitric-oxide synthase (eNOS) (44307M), and anti-eNOS antibodies (334600) were from Biosource International (Camarillo, CA, USA).

Preparation of rAAVs and Quantitation of Viral Titers

The rAAV plasmids carrying human *CD151*, *antiCD151*, or the green fluorescent protein (*GFP*) reporter gene were made as described previously (14,23–24).

The packing and production of the rAAV-GFP, rAAV-CD151, and rAAV-antiCD151 were carried out using a triple-plasmid cotransfection method in 293 cell lines. The plasmid pXX2 (for serotype 2) and the adenovirus helper plasmid pHelper were made and a total of 85 mg of plasmid DNA were used for transfection (the molar ratios of dsAAV-GFP, dsAAV-CD151, or dsAAV-antiCD151 to pXX2 and pHelper were 1:1:1). Then the single step gravity-flow column purification method was applied (25). The eluted rAAVs were divided into aliquots and stored at -80° C. The titer of vector particles was determined by the quantitative DNA dot-blot hybridization of DNase I-treated vector stocks.

Animal Preparation and Gene Delivery

Twenty-six purebred male pigs (Animal Resource Center, Huazhong Agriculture University, Wuhan, China), weighing 22–26 kg, 3 months of age, were housed at our institution for a minimum of 1 wk prior to use. They received normal swine food. The animals were randomized into four groups. Four normal pigs underwent no operation and served as the control group. The remaining 22 pigs served as three viral-administered groups, and underwent coronary artery ligation and received intramyocardial viral injection.

Briefly, the pigs were sedated with intramuscular diazepam (0.05 mg/kg), atropine (0.05 mg/kg), and ketamine (20 mg/kg), and then intubated. Sedation was maintained with sodium thiopental (2.5–4 mg/kg/h) and pancuronium (0.1–0.15 mg/kg/h). A limited left thoracotomy was performed aseptically through the fifth intercostal space, and a small incision was made in the pericardium. The heart was exposed and suspended in a pericardial sling. A silk suture was set at the immediate distal end of the second branch of the left anterior descending (LAD) coronary artery and ligated 20 min later. Coronary occlusion was confirmed by the presence of raised segment (ST) stages on the electrocardio-

gram and ventricular arrhythmias within the first 10 to 20 min after occlusion (ST is the part of an electrocardiogram immediately following the QRS complex and merging into the T wave). Simultaneously with the LAD ligation, all remaining animals received direct intramyocardial injection of rAAV-CD151, rAAV-antiCD151, and rAAV-GFP (1×10^{12} virions per pig, in 2 mL phosphate buffered saline, pH 7.4), respectively, in the ischemic area along the two sides of the ligated LAD coronary artery (10 sites for each animal and 5 for each side with ~1-cm interval). The injection sites were marked with India ink for subsequent identification. Experimental protocols complied with the *Guide for the Care and Use of Laboratory Animals* and were approved by the Chinese Academy of Sciences.

Assessment of the Regional Myocardial Perfusion

Regional myocardial perfusion was evaluated at 3 d and 8 wks after the viral administration by means of ^{13}N -labeled NH_3 positron emission computed tomography (^{13}N - NH_3 PET). The pigs were placed in the dorsal (supine) position and PET scans were performed with 15-cm axial field of view (DISCOVERY LS-GE, Milwaukee, WI, USA) over the cardiac region. PET images were acquired in 2D mode, starting 20 min after intravenous injections of 555 to 740 MBq (15 to 20 mCi) bolus of ^{13}N - NH_3 . During the PET scans, animals were maintained under general anesthesia as described above. Transaxial cardiac images were then reoriented into horizontal long-axis, vertical long-axis, and short-axis images with a thickness of 4.25 mm. Three axis views were analyzed further.

Echocardiographic Assessment of Regional Myocardial Function

The same zones for each animal were analyzed by echocardiography at 3 d and 8 wks after viral administration. The pigs were sedated and placed in the left lateral decubitus position, and standard two-dimensional and M-mode transthoracic images were obtained with a Vivid 7

Dimension echocardiographic machine (GE Healthcare, Waukesha, WI, USA) and a 1.5 to 4.0 MHz frequency transthoracic transducer. From the right parasternal approach, short-axis, midpapillary views were obtained at rest for 3 min. Regional wall thickening, myocardial contractile function, and wall motion were determined by a single experienced investigator in a blinded fashion. These images and parameters were recorded for subsequent review and analysis.

Immunohistochemistry Analysis and Data Acquisition

Heart tissue samples were taken from the region of the left ventricle around the previously marked sites 8 wks after viral administration and cut into 4- μm thick sections. Some sections were stained with hematoxylin and eosin (H-E). Some sections were used for immunohistochemical staining with vWF and SM α -actin antibodies, respectively, for capillaries and arterioles correspondingly.

The densities of capillaries and arterioles were evaluated according to the methods previously described (5,26). The five blood vessel-rich regions were selected, and the vessels within the 400 \times microscopic field of each region were counted by two blinded investigators without knowledge of groups. The densities of capillaries (positive vWF stain) and arterioles (positive SM α -actin stain) in each field were evaluated by counting vessels in a total of five high-powered fields (HPF) per region per heart under ocular micrometers (Olympus Optical Co. Ltd., Tokyo, Japan).

Measurement of Nitric Oxide Concentration

At 8 wks after vector administration, all five tissue samples were taken from the ischemic heart region in one pig around the previously marked sites. The levels of nitric oxide (NO) were measured using the NO detection kit (Jingmei, China) by following the protocol exactly as provided by the manufacturer. In brief, the sampled myocardial tissues were homogenized and reacted with nitrate re-

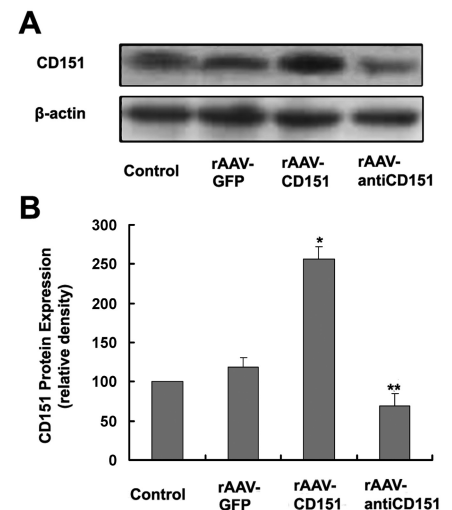


Figure 1. Myocardial expression of CD151 after *CD151* gene delivery. (A) Western blot analysis of CD151 and β -actin. β -actin was used as an internal control. (B) Quantitative analysis of CD151 protein expression. Results show a substantial increase of CD151 proteins in rAAV-CD151 group, but a decrease in the rAAV-antiCD151 group. Data are presented as mean \pm SEM ($n = 4-6$ per group). * $P < 0.05$ versus control and rAAV-GFP groups. ** $P < 0.05$ versus rAAV-GFP group.

ductase in the presence of cofactor. The NO concentration was calculated for these parameters as: $\text{NO } (\mu\text{mol/L}) = \text{Sample OD} / \text{Standard OD} \times 100$.

Western Blotting

All five tissue samples were taken from the ischemic heart region around the previously marked sites in one pig 8 wks after vector administration. To investigate the effects of rAAV-CD151 treatment on myocardial tissue protein expression, proteins were extracted, quantified, and separated by SDS-polyacrylamide gel electrophoresis (PAGE) as described previously (14). Western blots were probed with antibodies against CD151, phospho-FAK, FAK, PI3K, phospho-Akt, Akt, phospho-eNOS, eNOS, phospho-p38MAPK, p38MAPK, phospho-JNK, JNK, phospho-c-Jun, c-Jun, and β -actin. The intensities of the various protein bands were quantified by densitometry.

Statistical Analysis

Data were expressed as the mean \pm standard error of the mean (SEM). Comparisons of parameters were performed by one-way analysis of variance (ANOVA), followed by the Newman-Keuls test for unpaired data. Comparisons of parameters between two groups were made by unpaired Student *t* test. *P* values of <0.05 were regarded as statistically significant.

RESULTS

Overall Assessment

Of the total 26 pigs that entered the study, 22 pigs (control group, *n* = 4; rAAV-GFP group, *n* = 6; rAAV-CD151 group, *n* = 6; and rAAV-antiCD151 group, *n* = 6) survived throughout the study, without any clinical sign of toxicity. Four pigs died during the experimental surgery or at the stage of multiple analyses. The three viral administered groups (rAAV-GFP group, rAAV-CD151 group, and rAAV-antiCD151 group) exhibited evidence of myocardial infarction in the ligated distal LAD coronary artery region, as demonstrated by (1) a fixed defect in the LAD coronary artery zone of the $^{13}\text{N-NH}_3$ PET images, (2) a thinned, akinetic region of the left ventricle during echocardiography, and (3) large chaotic fibrous tissues, instead of normal regular cardiocytes, in the H-E staining of myocardial tissue.

CD151 Gene Delivery Increases the Expression of CD151 Proteins

Western blot analysis showed that the *in vivo* expression of CD151 proteins was increased significantly in the rAAV-CD151 group compared with the control and rAAV-GFP groups, but decreased in the rAAV-antiCD151 group (Figure 1A, B). There was no significant difference between the control and rAAV-GFP groups in the CD151 expression. These results indicate that rAAV-mediated CD151 gene delivery promotes the CD151 protein expression in myocardial tissue.

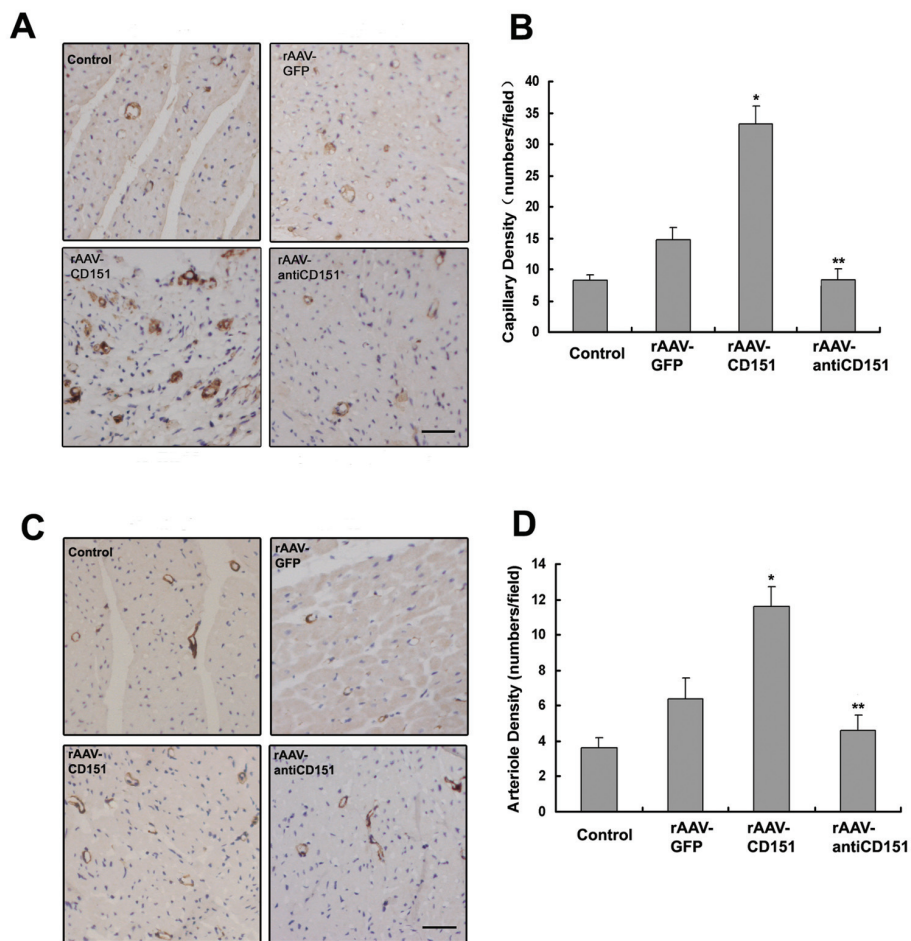


Figure 2. Overexpression of CD151 increases the densities of capillaries and arterioles. (A) Immunohistochemical staining of capillaries with antibody to von Willebrand factor (vWF). The ECs are stained in brown. Bar represents 50 μm . (B) Density of myocardial capillary. (C) Immunohistochemical staining of arterioles with antibody to SM α -actin. The smooth muscle cells are indicated in brown. Bar represents 50 μm . (D) Density of myocardial arteriole. Data are mean \pm SEM (*n* = 4–6 per group). **P* < 0.05 versus control and rAAV-GFP groups. ***P* < 0.05 versus rAAV-GFP group.

rAAV-CD151 Increases the Densities of Capillaries and Arterioles

Formation of capillaries and arterioles was evaluated by vWF-positive and SM α -actin-positive vessels at 8 wks after the viral transduction (Figure 2). The CD151 gene, transferred to ischemic myocardium, enhanced the densities of capillaries and arterioles compared with the control group and the rAAV-GFP group. In contrast, capillary and arteriole densities were decreased in the rAAV-antiCD151 group compared with the rAAV-GFP group. These findings indicate that CD151 gene delivery increases

the formation of capillaries and arterioles, and enhances both angiogenesis as well as arteriogenesis responses.

Effects of rAAV-CD151 Delivery on Myocardial Perfusion

The $^{13}\text{N-NH}_3$ PET image data was used to display the myocardial perfusion and the severity of myocardial ischemia. The control group for myocardial perfusion in normal pigs exhibited no detectable defect (Figure 3A). In the three viral transduced groups, PET images obtained at 3 d after viral transduction displayed similar myocardial perfusion with a

characteristic perfusion defect, mainly at apical, anterior, and some septal regions. At 8 wks after viral administration, the rAAV-CD151 group exhibited significantly improved myocardial perfusion compared with the rAAV-GFP group. This improvement was found at the anterior and septal regions. However, perfusion in the rAAV-antiCD151 group worsened and most images revealed hyperdispersion and decreased perfusion (Figure 3B–D).

Together, these data indicate that rAAV-CD151 treatment significantly promotes the myocardial blood perfusion and reduces myocardial ischemia.

Effects of rAAV-CD151 Delivery on Myocardial Function

The effects of rAAV-CD151 delivery on the myocardial function were examined by echocardiography. Myocardial function and regional wall motion were reduced 3 d after vector administration in all three viral administration groups compared with the control group (Figure 4A–D). There was no significant difference of wall thickness in these four groups (Figure 4E, F).

In contrast, by 8 wks after vector administration, the increased left ventricular ejection fraction (LVEF%) and left ventricular shortening fraction (LVFS%) were found in the rAAV-CD151 group compared with the rAAV-GFP group, which showed marked improvement in myocardial contractile function (Figure 4A, B). The regional wall motion, verified by anterior lateral wall systolic thickening fraction (Δ ALWT%) and interventricular septal systolic thickening fraction (Δ IVST%), showed further improvement in the rAAV-CD151 group compared with the rAAV-GFP group (Figure 4C, D). The septal and anterior lateral wall diastolic thickness, according to anterior lateral wall diastolic thickness (ALWTd) and interventricular septal diastolic thickness (IVSTd), both were increased in the rAAV-CD151 group (Figure 4E, F). LVEF% and LVFS% were decreased in the rAAV-antiCD151 group compared with rAAV-GFP group. The rAAV-antiCD151 group

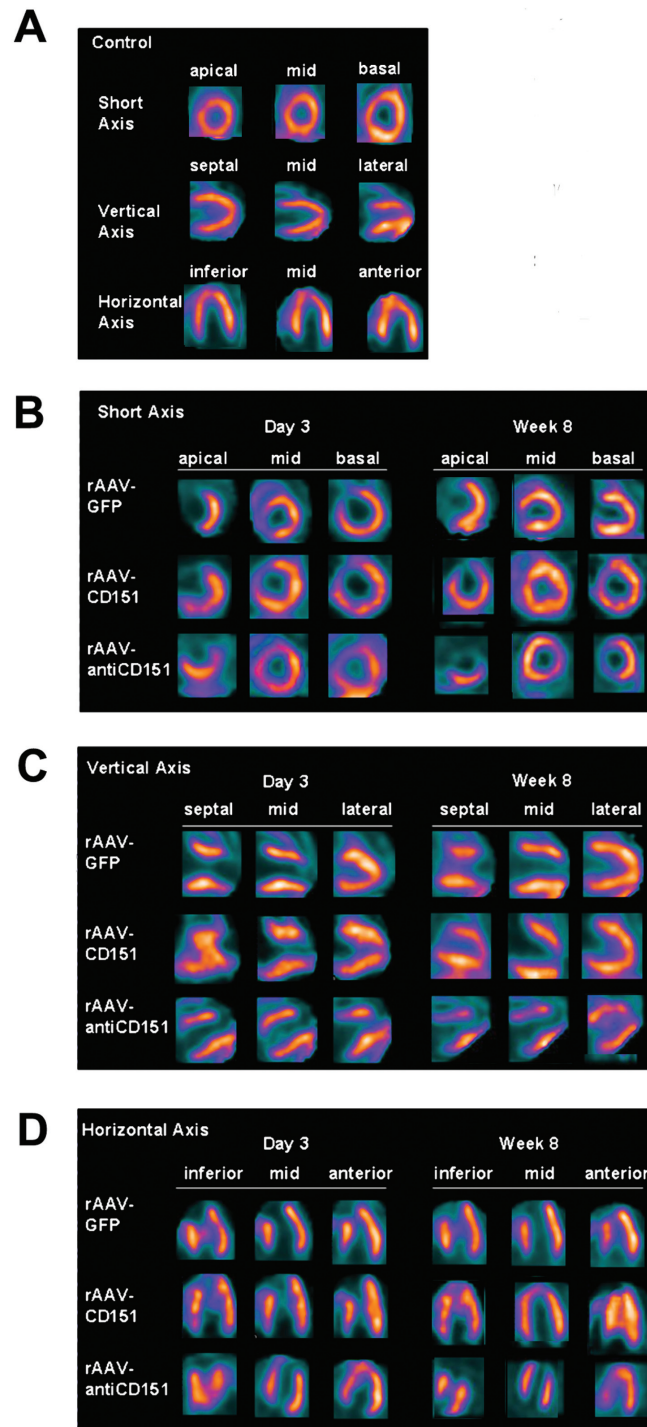


Figure 3. rAAV-CD151 transfection enhances myocardial perfusion and reduces ischemia. (A) $^{13}\text{N-NH}_3$ PET images of the control group. (B–D) $^{13}\text{N-NH}_3$ PET images of the rAAV-GFP, rAAV-CD151, and rAAV-antiCD151 groups in three axes. (B) Short axis images. (C) Vertical axis images. (D) Horizontal axis images. The control group exhibited no detectable defect. At 3 d after viral transduction, three viral transduced groups displayed similar myocardial perfusion. At 8 wks after viral administration, the rAAV-CD151 group exhibited significantly improved myocardial perfusion compared with the rAAV-GFP group. In contrast, rAAV-antiCD151 group revealed decreased perfusion.

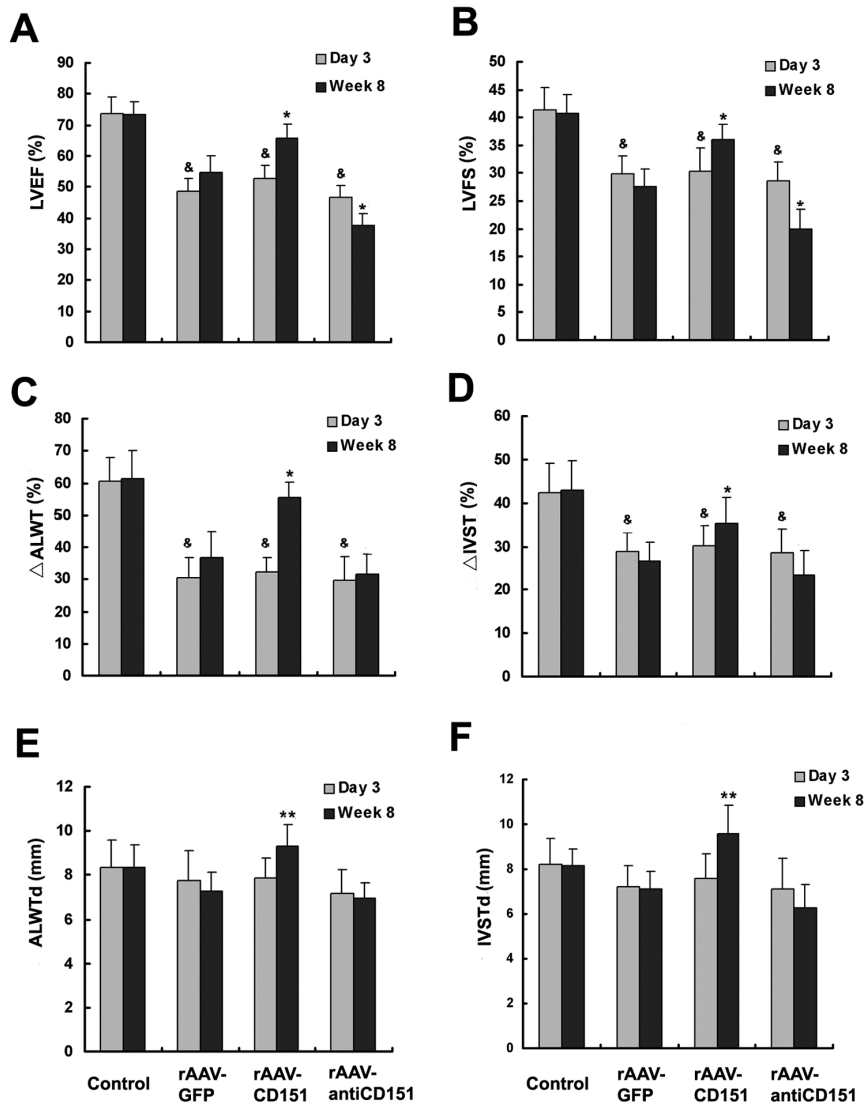


Figure 4. CD151 gene delivery improves myocardial function. (A) and (B) LVEF% and LVFS% showed myocardial contractile function was improved in the rAAV-CD151 group, but decreased in the rAAV-antiCD151 group 8 wks after vector administration. LVEF, left ventricular ejection fraction; LVFS, left ventricular shortening fraction. (C) and (D) ΔALWT% and ΔIVST% showed the regional motion of anterior lateral and interventricular septal wall was improved in the rAAV-CD151 group 8 wks after vector administration. ΔALWT, anterior lateral wall systolic thickening fraction; ΔIVST, interventricular septal systolic thickening fraction. (E) and (F) ALWTd and IVSTd showed the thickness of anterior lateral and interventricular septal wall was increased in the rAAV-CD151 group 8 wks after vector administration. ALWTd, anterior lateral wall diastolic thickness; IVSTd, interventricular septal diastolic thickness. Data are presented as mean ± SEM (n = ~4-6 per group). &P < 0.05 versus control group; *P < 0.05 versus control and rAAV-GFP groups; **P < 0.05 versus rAAV-GFP group.

showed deteriorated heart function. However, there was no significant difference in septal and anterior lateral wall diastolic thickness between rAAV-

antiCD151 group and rAAV-GFP group. These results demonstrate that rAAV-CD151 transduction results in enormous improvement of myocardial contractile

function and wall motion, and significant increases in wall thickness.

Effects of rAAV-CD151 Delivery on Signaling Pathway

The effects of rAAV-CD151 delivery on the FAK, MAPKs, and PI3K/Akt/eNOS signaling pathways were examined. Western blot analysis showed CD151 expression significantly elevated phosphorylation-dependent activation of signaling components, such as FAK, ERK1/2, JNK, and c-Jun (Figure 5A-D). Both phospho-FAK397 and phospho-FAK925 were increased in the rAAV-CD151 group. By contrast, the level of phospho-p38MAPK proteins demonstrated no significant difference among the four groups, which suggests overexpression of CD151 did not affect the activity of p38MAPK protein.

Our study demonstrates that CD151 also activates the PI3K/Akt/eNOS pathway. PI3K expression, phospho-Akt, and phospho-eNOS protein levels were increased in the CD151-transfected myocardium and the NO concentration also was higher, compared with both the control group and the rAAV-GFP group (Figure 5E-G). In contrast, such changes all were reversed in the rAAV-antiCD151 group. Taken together, these results suggest that overexpression of CD151 activates FAK, ERK1/2, JNK, and PI3K/Akt/eNOS signaling pathways.

DISCUSSION

Blood flow tends to depend more on arterioles than on capillaries, which lack vascular smooth muscle cells (2-5). An arteriogenesis response, which consists of the formation of new arterioles, can occur. These vessels, implicated in arteriogenesis, are microvascular, thin-walled conduits composed of an endothelial lining, an internal elastic lamina, and one or two layers of smooth muscle cells. These arteries have the ability to provide enhanced perfusion to the jeopardized ischemic regions (4). In addition, because collateral arteries require a functional capillary network for effective exchange of oxygen and nutrients, angiogenesis

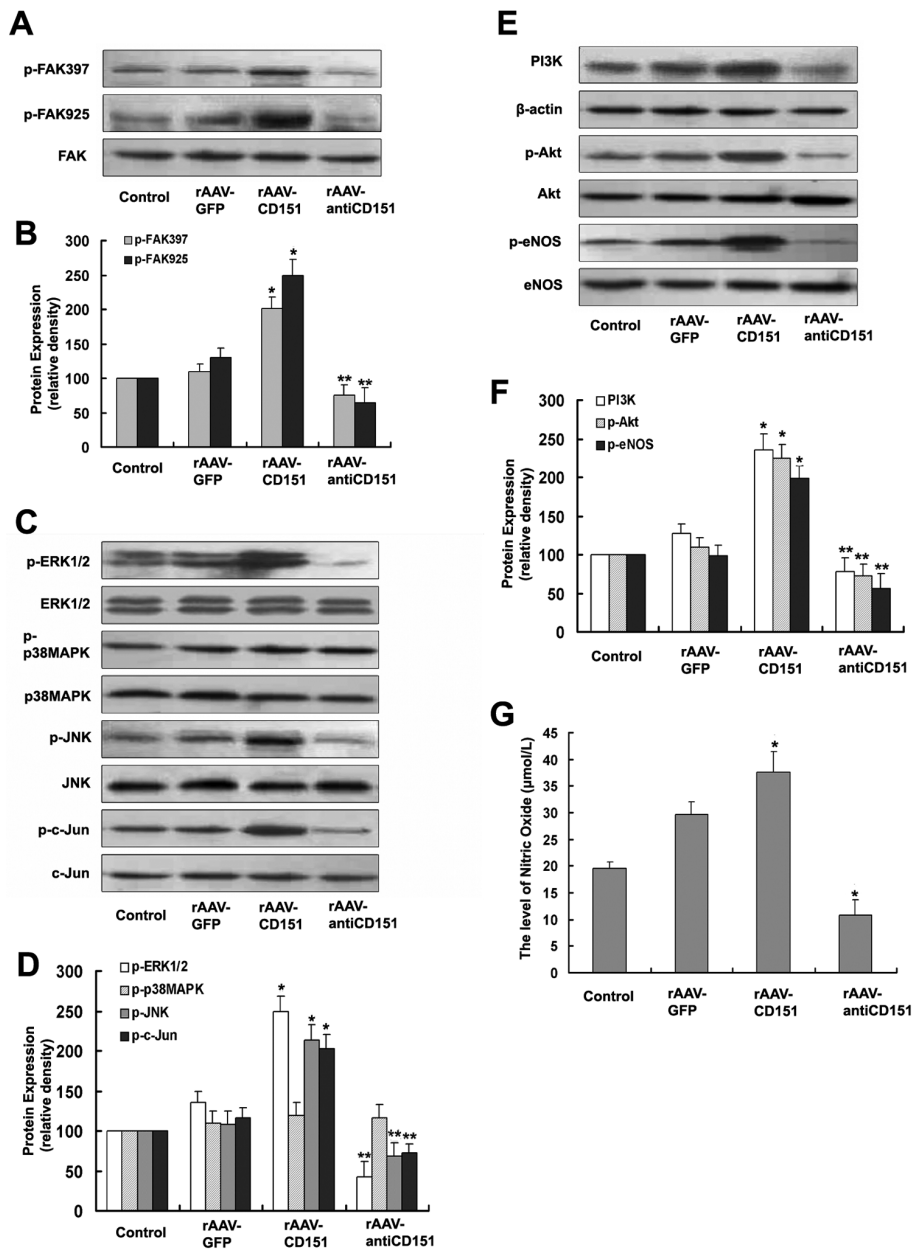


Figure 5. CD151 activates MAPKs and PI3K signaling pathways. (A) and (B) Levels of FAK, phospho-FAK (Tyr397), and phospho-FAK (Tyr925). (C) and (D) Levels of ERK1/2, phospho-ERK1/2, JNK, phospho-JNK, c-Jun, phospho-c-Jun, p38MAPK, and phospho-p38MAPK. (E) and (F) The levels of PI3K, Akt, phospho-Akt, eNOS, and phospho-eNOS. (G) The level of myocardial NO. Data are presented as mean \pm SEM ($n = 4-6$ per group). * $P < 0.05$ versus control and rAAV-GFP groups; ** $P < 0.05$ versus rAAV-GFP group.

and arteriogenesis are connected tightly and both are important to myocardial perfusion (1).

Our previous studies have indicated that *in vivo* CD151 gene delivery increases the number of capillaries and induces an

angiogenesis response in different models (14,15). These previous studies, however, did not address whether CD151 induces arteriogenesis or promotes myocardial perfusion. The present immunohistological data suggest CD151 gene delivery in-

duces both angiogenesis and arteriogenesis as evaluated by the increases in capillary density and SM-coated arteriole density, respectively. Further data from $^{13}\text{N-NH}_3$ PET imaging and echocardiography demonstrated that CD151-induced neovascularization can efficiently enhance the myocardial perfusion and ameliorate the regional myocardial dysfunction. Herein, rAAV-mediated *CD151* gene delivery promotes the functional neovascularization, resulting in a marked enhancement of formation of neocapillaries and new arterioles and an increase in the regional blood flow recovery.

The extensive analysis of the CD151 signaling revealed some interesting observations. Activations of FAK, Src, p38 MAPK, JNK, and c-Jun, but not ERK1/2, are required for the CD151-dependent enhancement of cell migration and cell-to-cell adhesion in MelJuSo melanoma cells (21). However, other studies found that the overexpression of CD151 has no effect on the adhesion-dependent activation of FAK, but specifically attenuates the adhesion-dependent activation of ERK1/2 and PKB/c-Akt (27,28). Furthermore, Takeda *et al.* showed that the adhesion-dependent activation of PKB/c-Akt and eNOS is diminished in CD151-null MLECs while the activities of ERK, p38 MAPK, FAK, and Src are unaltered (12). The present study analyzed CD151 delivery and demonstrated that CD151 transduces signals leading to the activation of MAPKs and PI3K/Akt/eNOS pathways. FAK (phospho-FAK397 and phospho-FAK925), MAP kinases (phospho-ERK1/2 and phospho-JNK), Akt (phospho-Akt), and eNOS (phospho-eNOS) all were activated in the rAAV-CD151 group. As JNK plays a role of upstream effectors for c-Jun, the phospho-c-Jun protein level was increased and c-Jun was activated further. We also found that the PI3K protein level and NO production were upregulated by *CD151* gene transfer. In contrast, when the expression of CD151 was reduced, the activities of these signaling proteins were decreased significantly.

The FAK pathway is one of the most important integrin-mediated signaling

- alpha3 beta1 integrin localized at endothelial lateral junctions. *J. Cell Biol.* 141:791–804.
11. Zhang XA, *et al.* (2002) Function of the tetraspanin CD151-alpha6beta1 integrin complex during cellular morphogenesis. *Mol. Biol. Cell.* 13:1–11.
 12. Takeda Y, *et al.* (2007) Deletion of tetraspanin Cd151 results in decreased pathologic angiogenesis *in vivo* and *in vitro*. *Blood.* 109:1524–32.
 13. Zheng ZZ, Liu ZX. (2007) Activation of the phosphatidylinositol 3-kinase/ protein kinase Akt pathway mediates CD151- induced endothelial cell proliferation and cell migration. *Int. J. Biochem Cell Biol.* 39:340–8.
 14. Lan RF, Liu ZX, Liu XC, Song YE, Wang DW. (2005) CD151 promotes neovascularization and improves blood perfusion in a rat hind-limb ischemia model. *J. Endovasc. Ther.* 12:469–78.
 15. Zheng Z, Liu Z. (2006) CD151 gene delivery activates PI3K/Akt pathway and promotes neovascularization after myocardial infarction in rats. *Mol. Med.* 12:214–20.
 16. Lammerding J, Kazarov AR, Huang H, Lee RT, Hemler ME. (2003) Tetraspanin CD151 regulates alpha6beta1 integrin adhesion strengthening. *Proc. Natl. Acad. Sci. U. S. A.* 100:7616–21.
 17. Yauch RL, Berditchevski F, Harler MB, Reichner J, Hemler ME. (1998) Highly stoichiometric, stable, and specific association of integrin alpha3beta1 with CD151 provides a major link to phosphatidylinositol 4-kinase, and may regulate cell migration. *Mol. Biol. Cell.* 9:2751–65.
 18. Nishiuchi R, *et al.* (2005) Potentiation of the ligand-binding activity of integrin alpha3beta1 via association with tetraspanin CD151. *Proc. Natl. Acad. Sci. U. S. A.* 102:1939–44.
 19. Zhang XA, Bontrager AL, Hemler ME. (2001) Transmembrane-4 superfamily proteins associate with activated protein kinase C (PKC) and link PKC to specific beta(1) integrins. *J. Biol. Chem.* 276:25005–13.
 20. Klosek SK, *et al.* (2005) CD151 forms a functional complex with c-Met in human salivary gland cancer cells. *Biochem. Biophys. Res. Commun.* 336:408–16.
 21. Hong IK, *et al.* (2006) Homophilic interactions of Tetraspanin CD151 up-regulate motility and matrix metalloproteinase-9 expression of human melanoma cells through adhesion-dependent c-Jun activation signaling pathways. *J. Biol. Chem.* 281:24279–92.
 22. Zheng ZZ, Liu ZX. (2007) CD151 gene delivery increases eNOS activity and induces ECV304 migration, proliferation and tube formation. *Acta. Pharmacol. Sin.* 28:66–72.
 23. Lan R, Liu Z, Song Y, Zhang X. (2004) Effects of rAAV-CD151 and rAAV- antiCD151 on the migration of human tongue squamous carcinoma cell line Tca8113. *J. Huazhong Univ. Sci. Technol. Med. Sci.* 24:556–9.
 24. Wang T, *et al.* (2004) Recombinant adeno-associated virus-mediated kallikrein gene therapy reduces hypertension and attenuates its cardiovascular injuries. *Gene Ther.* 11:1342–50.
 25. Auricchio A, Hildinger M, O'Connor E, Gao GP, Wilson JM. (2001) Isolation of highly infectious and pure adeno-associated virus type 2 vectors with a single-step gravity-flow column. *Hum. Gene Ther.* 12:71–6.
 26. Weidner N, *et al.* (1992) Tumor angiogenesis: a new significant and independent prognostic indicator in early-stage breast carcinoma. *J. Natl. Cancer Inst.* 84:1875–87.
 27. Berditchevski F, Odintsova E, Sawada S, Gilbert E. (2002) Expression of the palmitoylation-deficient CD151 weakens the association of alpha 3 beta 1 integrin with the tetraspanin-enriched microdomains and affects integrin-dependent signaling. *J. Biol. Chem.* 277:36991–7000.
 28. Sawada S, Yoshimoto M, Odintsova E, Hotchin NA, Berditchevski F. (2003) The tetraspanin CD151 functions as a negative regulator in the adhesion-dependent activation of Ras. *J. Biol. Chem.* 278:26323–6.
 29. Kohno M, Hasegawa H, Miyake M, Yamamoto T, Fujita S. (2002) CD151 enhances cell motility and metastasis of cancer cells in the presence of focal adhesion kinase. *Int. J. Cancer.* 97:336–43.
 30. Chen HC, Appeddu PA, Isoda H, Guan JL. (1996) Phosphorylation of tyrosine 397 in focal adhesion kinase is required for binding phosphatidylinositol 3-kinase. *J. Biol. Chem.* 271:26329–34.
 31. Clark EA, Hynes RO. (1997) 1997 keystone symposium on signal transduction by cell adhesion receptors. *Biochim. Biophys. Acta.* 1333:R9–16.
 32. Graf K, *et al.* (1997) Mitogen-activated protein kinase activation is involved in platelet-derived growth factor- directed migration by vascular smooth muscle cells. *Hypertension.* 29:334–9.
 33. Kyriakis JM, Avruch J. (2001) Mammalian mitogen-activated protein kinase signal transduction pathways activated by stress and inflammation. *Physiol. Rev.* 81:807–69.
 34. Adya R, Tan BK, Punn A, Chen J, Randeve HS. (2008) Visfatin induces human endothelial VEGF and MMP-2/9 production via MAPK and PI3K/Akt signalling pathways: novel insights into visfatin-induced angiogenesis. *Cardiovasc. Res.* 78:356–65.
 35. Lee SJ, *et al.* (2006) Fractalkine stimulates angiogenesis by activating the Raf-1/MEK/ERK- and PI3K/Akt/eNOS-dependent signal pathways. *Am. J. Physiol. Heart Circ. Physiol.* 291:H2836–46.
 36. Mehta VB, Besner GE. (2007) HB-EGF promotes angiogenesis in endothelial cells via PI3-kinase and MAPK signaling pathways. *Growth Factors.* 25:253–63.
 37. Sugiura T, Berditchevski F. (1999) Function of alpha3beta1- tetraspanin protein complexes in tumor cell invasion. Evidence for the role of the complexes in production of matrix metalloproteinase 2 (MMP-2). *J. Cell Biol.* 146:1375–89.